

## **The Thermodynamics of the Divalent Metal Fluorides. II. Heat Capacity of the Fast Ion Conductor BaSnF<sub>4</sub> from 7 to 345 K<sup>1</sup>**

**J. E. Callanan,<sup>2</sup> R. D. Weir,<sup>3</sup> and E. F. Westrum, Jr.<sup>4</sup>**

---

The heat capacity of the fast ion conductor BaSnF<sub>4</sub> was measured over the temperature range  $7 < T < 345$  K using adiabatic calorimetry. Our results show that a phase transition is not present. However, an anomalous rise in the molar heat capacity,  $C_{p,m}$ , occurs in the region  $210 < T < 310$  K; the entropy change of this rise amounts to  $\Delta S/R = 0.112$ . This anomaly coincides with the temperature range where a break in the slope of the electrical conductivity has been observed, which results in a threefold decrease in the activation energy required in the temperature region above the break at 272 K. Standard molar thermodynamic functions are presented at selected temperatures from 5 to 345 K.

---

**KEY WORDS:** barium tetrafluorostannate; fast ion conductor; heat capacity; low temperature.

### **1. INTRODUCTION**

A solid with an ionic conductivity that compares with that of a molten salt is referred to as a fast ion conductor. These solid electrolytes are of technological significance because of their applications in electronic devices and batteries. It is well known that the electrolytic oxides such as ZrO<sub>2</sub> exhibit high conduction only at temperatures above 870 K [1, 2], whereas the isostructural fluorides exhibit significant anionic conduction at temperatures down to 300 K [3, 4]. In addition, the fast ion fluoride elec-

---

<sup>1</sup> Paper presented at the Tenth Symposium on Thermophysical Properties, June 20–23, 1988, Gaithersburg, Maryland, U.S.A.

<sup>2</sup> Chemical Engineering Science Division, National Institute of Standards and Technology (formerly National Bureau of Standards), Boulder, Colorado 80303, U.S.A.

<sup>3</sup> Department of Chemistry and Chemical Engineering, Royal Military College of Canada, Kingston, Ontario K7K 5L0, Canada.

<sup>4</sup> Department of Chemistry, University of Michigan, Ann Arbor, Michigan 48109-1055, U.S.A.

trolytes are often electronic insulators, which is an important property for their use as electrolytes in electrochemical cells [5]. Because of the use of fluoride electrolytes as thin films in galvanic cells, fluorine ion-specific electrodes, and gas detectors [6–8], considerable experimental work has been directed at fluorides with the fluorite-type structure, which includes the family  $M\text{SnF}_4$ , where  $M = \text{Pb}, \text{Ba}, \text{Sr}$ .

Several allotropic forms of  $\text{PbSnF}_4$  are known to exist at temperatures above 273 K [4, 9–12]. The normal  $\alpha$  phase at room temperature, which is dependent upon the method of preparation, has a monoclinic, sometimes called a pseudomonoclinic, structure with space group  $P_{2/n}$ , which is stable to about 353 K. The  $\beta$  phase, stable from about 353 to 623 K, is tetragonal with space group  $P_{4/nmm}$  [10–12]. When  $\text{PbSnF}_4$  is prepared via the dry method, the  $\alpha$  phase appears only after annealing [11]. The  $\gamma$  phase, which has a fluorite structure with space group  $F_{m3m}$ , is stable above 623 K up to fusion around 661 K [4, 10–12]. The heat capacity of  $\text{PbSnF}_4$  was recently measured by us over the range  $10.3 < T < 352$  K by adiabatic calorimetry [13]. A subtle anomaly in the heat capacity was detected between 130 and 160 K, which correlates nicely with the nuclear magnetic resonance (nmr) work by Chadwick et al. [14], whose results show a gentle drop in the  $^{19}\text{F}$  spin-lattice relaxation time in that temperature region.

The solid electrolyte  $\text{BaSnF}_4$  has also been shown to be a good fluoride ion conductor, with a conductivity intermediate between that of  $\text{PbSnF}_4$  and that of  $\text{TlBiF}_4$  [15] and an activation energy that is one of the lowest observed for fluoride ion conductors [3, 15]. Between room temperature and 693 K,  $\text{BaSnF}_4$  is isomorphous with the tetragonal structure of  $\beta\text{-PbSnF}_4$ . At 293 K, the lattice parameters of  $\text{BaSnF}_4$  were found to be  $a = 0.43564$  and  $c = 1.1289$  nm with  $Z = 2$  and a space group  $P_{4/nmm}$  or No. 129  $D_{4h}^7$  [10, 15, 16]. X-Ray diffraction studies of the thermal expansion coefficients from 77 to 685 K show no phase transition and the  $\text{BaSnF}_4$  decomposing above 673 K [15, 16].

In probing the conduction mechanism in  $\text{PbSnF}_4$  and  $\text{BaSnF}_4$  using nmr techniques, Chadwick et al. [14] found the behavior of the relaxation to be broadly similar in the two compounds, although some differences in detail were noted. Heat capacity data have not been reported for  $\text{BaSnF}_4$ , and because these should assist in understanding the conduction mechanism in the compound, their measurement was undertaken by us using adiabatic calorimetry from about 7 to 345 K.

## 2. EXPERIMENTAL

The  $\text{BaSnF}_4$  sample was prepared by a solid-state reaction of a 1:1 stoichiometric mixture of  $\text{BaF}_2$  and  $\text{SnF}_2$ , which was ground to a fine

powder in an agate mortar and pestle. Pellets were pressed from the powder within a stainless-steel die and then loaded into a specially designed copper tube evacuated to  $0.133 \times 10^{-5}$  kPa. Sintering occurred by heating the copper inside an evacuated silica tube for 12 h at 523 K. Following the sintering process, the copper tube showed no visible signs of reaction with the pellets. Annealing was carried out in two stages, unlike that done for  $\text{PbSnF}_4$  [13]. The  $\text{BaSnF}_4$  pellets were annealed for 1 h at 473 K followed by 1 h at 773 K. Then they were allowed to cool to room temperature, where they remained until they were loaded into the calorimeter. Once loaded, the sample was cooled to 5.7 K for heat capacity measurements. The X-ray powder pattern at room temperature confirmed the structure of the sample as the tetragonal phase  $\beta$ -phase  $\text{BaSnF}_4$ , in agreement with literature data [15].

The calorimetric results were determined using the Mark XIII cryostat, which is an upgraded version of the Mark II cryostat already described [17]. A guard shield was incorporated around the adiabatic shield. A capsule-type platinum resistance thermometer (laboratory designation A-5) was used for temperature measurements. The thermometer was calibrated at the U.S. National Bureau of Standards (NBS) against the IPTS-1948 (as revised in 1960) [18] for temperatures above 90 K, against the NBS provisional scale from 10 to 90 K, and by the technique of McCracken and Chang [19] below 10 K. These calibrations are judged to reproduce thermodynamic temperatures to within 0.03 K between 10 and 90 K and within 0.04 above 90 K [20]. Measurements of mass, current, voltage, and time are based upon calibrations done at the NBS. The heat capacities from about 10 to 352 K were acquired with the assistance of a computer [21, 22], which was programmed for a series of determinations. During the drift periods, both the calorimeter temperature and the first and second derivatives of temperature with respect to time were recorded to establish the equilibrium temperature of the calorimeter before and after the energy input. While the calorimeter heater was on, the heater current and voltage as well as the duration of the heating interval were determined. Also recorded was the apparent heat capacity of the system, which included the calorimeter, heater, thermometer, and sample.

The gold-plated copper calorimeter (laboratory designation W-UK) without internal vanes was loaded with the  $\text{BaSnF}_4$  sample, which was in the form of a single cylindrical-shaped rod. The calorimeter vessel contained a reentrant well for the heater and thermometer that was located off center, thereby allowing the accommodation of massive samples. After loading, the removable lid with a diameter equal to that of the calorimeter vessel was soldered in place using a low-melting point (bismuth/tin/indium) solder. The calorimeter was then evacuated through the

stainless-steel seal-off tip provided in the lid. Helium gas was admitted to the vessel to a pressure of 3.7 kPa at 295 K to facilitate thermal equilibrium. The vessel was then sealed by means of the seal-off tip, which was crimped tightly, cut, and soldered.

The empty calorimeter vessel has a mass of 18.70 g and an internal volume of  $17.0 \times 10^{-6} \text{ m}^3$ . Buoyancy corrections were calculated on the basis of the crystallographic density of  $5145.9 \text{ kg} \cdot \text{m}^{-3}$  from the X-ray diffraction studies on the salt [10, 15]. The mass of  $\text{BaSnF}_4$  amounted to 15.959353 g or 0.04806837 mol based on its molar mass of  $332.0136 \text{ g} \cdot \text{mol}^{-1}$  calculated from the 1983 IUPAC recommended atomic masses of the elements.

### 3. RESULTS

The experimental molar heat capacities,  $C_{p,m}$ , of our  $\text{BaSnF}_4$  sample are presented in Table I, where the results are given in order of increasing temperature. The measurements were made in one series beginning at 5.7 K and ending at 349 K. The probable errors in heat capacity drop from about

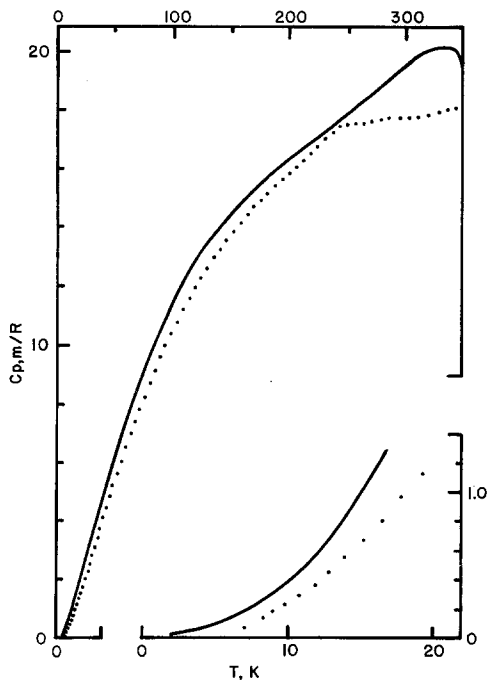


Fig. 1. The quantity  $C_{p,m}/R$  for  $\text{BaSnF}_4$  (this work;  $\cdots$ ) and  $\text{PbSnF}_4$  (Ref. 13;  $\text{—}$ ).

**Table I.** Experimental Molar Heat Capacity of BaSnF<sub>4</sub>  
 (Molar Mass = 332.014 g · mol<sup>-1</sup>,  $R = 8.3144 \text{ J} \cdot \text{K}^{-1} \cdot \text{mol}^{-1}$ )

$T$ (K)	$C_{p,m}/R$	$T$ (K)	$C_{p,m}/R$
7.01	0.08072	104.12	10.83
8.25	0.1432	109.13	11.22
8.98	0.1832	114.17	11.60
9.81	0.2293	119.22	11.96
10.75	0.2911	124.53	12.32
11.82	0.3697	130.10	12.68
12.90	0.4579	135.69	13.02
13.99	0.5578	141.28	13.33
15.22	0.6803	146.89	13.61
16.57	0.8248	152.52	13.89
17.93	0.9802	158.13	14.15
19.31	1.146	163.75	14.41
20.84	1.335	169.66	14.68
22.50	1.551	175.81	14.94
24.16	1.773	181.97	15.18
25.85	2.003	188.13	15.42
27.69	2.256	194.30	15.65
29.66	2.528	200.47	15.88
31.64	2.803	206.64	16.08
33.82	3.109	212.82	16.29
36.18	3.435	219.00	16.53
38.56	3.761	225.17	16.78
41.14	4.106	231.34	17.03
43.91	4.477	237.53	17.24
46.70	4.844	243.48	17.55
49.74	5.236	249.98	17.45
53.03	5.648	257.23	17.51
56.34	6.061	264.49	17.59
59.91	6.543	271.73	17.65
63.79	6.959	278.97	17.73
67.65	7.392	286.73	17.78
71.78	7.825	294.99	17.76
76.14	8.281	303.23	17.75
80.54	8.743	311.51	17.78
84.96	9.194	319.78	17.88
89.41	9.622	328.03	18.00
94.13	10.03	336.31	18.06
99.12	10.44	344.60	18.08

**Table II.** Standard Molar Thermodynamic Functions for BaSnF<sub>4</sub>  
 {Molar Mass = 332.014 g · mol<sup>-1</sup>; P<sup>0</sup> = 101.325 kPa; R = 8.3144 J · K<sup>-1</sup> · mol<sup>-1</sup>;  
 $\Phi_m^0(T, 0)^{\text{def}} = -\Delta_0^T H_m^0(T)/T + \Delta_0^T S_m^0(T); \Delta_0^T X(T) = [X(T) - X(0)]$ }

<i>T</i> (K)	<i>C<sub>p,m</sub></i> / <i>R</i>	$\Delta_0^T S_m^0(T)/R$	$\Delta_0^T H_m^0(T)/R$ (K)	$\Phi_m^0/R$
5	(0.031)	(0.010)	(0.040)	(0.0024)
10	0.243	0.084	0.631	0.0207
15	0.656	0.254	2.80	0.0672
20	1.233	0.520	7.50	0.1451
25	1.882	0.864	15.27	0.2433
30	2.579	1.267	26.42	0.3864
35	3.278	1.716	41.06	0.5429
40	3.953	2.197	59.14	0.7188
45	4.621	2.701	80.58	0.9106
50	5.270	3.221	105.3	1.115
55	5.924	3.754	133.3	1.331
60	6.545	4.296	164.5	1.555
65	7.130	4.843	198.7	1.787
70	7.654	5.391	235.6	2.025
75	8.164	5.936	275.2	2.267
80	8.692	6.480	317.3	2.514
85	9.195	7.022	362.0	2.763
90	9.674	7.561	409.2	3.015
95	10.11	8.096	458.7	3.268
100	10.51	8.625	510.2	3.523
105	10.90	9.147	563.7	3.778
110	11.29	9.663	619.2	4.034
120	12.02	10.68	735.8	4.546
130	12.68	11.66	859.3	5.056
140	13.25	12.63	989.0	5.562
150	13.76	13.56	1124.0	6.065
160	14.25	14.46	1264.1	6.561
170	14.71	15.34	1409.0	7.052
180	15.11	16.19	1558.1	7.536
190	15.49	17.02	1711.1	8.014
200	15.86	17.82	1867.8	8.484
210	16.19	18.61	2028.0	8.948
220	16.57	19.37	2191.8	9.404
230	16.98	20.11	2359.5	9.854
240	17.38	20.84	2531.3	10.30
250	17.53	21.56	2706.1	10.73
260	17.56	22.25	2881.4	11.16
270	17.64	22.91	3057.4	11.59
280	17.74	23.55	3234.3	12.00
290	17.78	24.18	3411.9	12.41
300	17.77	24.78	3589.7	12.81
310	17.78	25.36	3767.4	13.21
320	17.87	25.93	3945.6	13.60
330	18.02	26.48	4125.1	13.98
340	18.07	27.02	4305.6	14.36
345	18.08	27.28	4396.0	14.54
298.15	17.77 ± 0.03	24.67 ± 0.04	3556.8 ± 5.4	12.74 ± 0.02

1% at 10 K to less than 0.15% at temperatures above 30 K. The heat capacity of the sample amounted to 70% down to 40% of the total heat capacity of the sample plus the calorimeter vessel.

Shown in Fig. 1 is the  $C_{p,m}/R$  (where  $R$  is the gas constant) plot for  $\text{BaSnF}_4$  from 7 to 345 K, shown as the dots. One anomaly appears in the heat capacity curve.

The standard molar thermodynamic functions are presented at selected temperatures in Table II. The heat capacities below 8 K were obtained by fitting our experimental values below 20 K to the limiting form of the Debye equation, using a plot of  $C_{p,m}/T$  against  $T^2$  and extrapolating to 0 K. Because the temperatures in this work were not low enough to reach the linear region below the maximum in a plot of  $C_{p,m}/T^3$  against  $T^2$ , this relationship could not be used for the extrapolation.

#### 4. DISCUSSION

The course followed by the  $C_{p,m}/R$  for the  $\text{BaSnF}_4$  salt in the region of the anomaly is shown in Fig. 2 in an expanded plot. The smooth background curve drawn beneath the peak is given as the dashed line, which defines the temperature region of the anomaly as  $210 < T < 310$  K. The value of  $\Delta S$  associated with the area between the background and the experimental curves amounts to  $0.112 R$  and the difference between the  $C_{p,m}/R$  values of the two curves at 250 K is about 3% of the experimental  $C_{p,m}/R$  value.

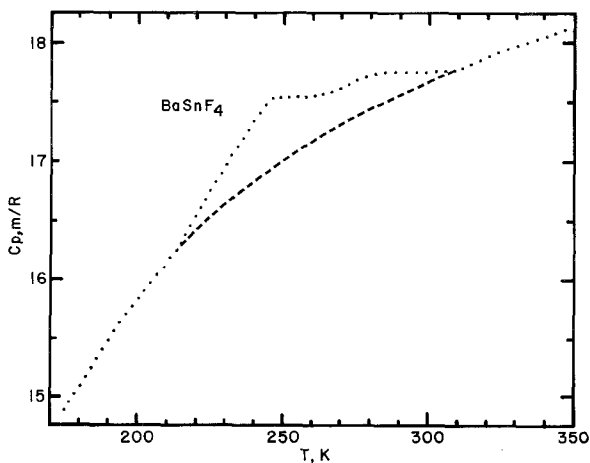


Fig. 2. The quantity  $C_{p,m}/R$  for  $\text{BaSnF}_4$  in the region of the anomaly. Experimental,  $\cdots$ ; smoothed background curve,  $---$ .

The heat capacity of  $\text{PbSnF}_4$  [13] is also shown in Fig. 1 for comparison with that of  $\text{BaSnF}_4$ . The rise in the heat capacity for the  $\text{PbSnF}_4$  salt around 300 K and its subsequent decrease by 350 K are associated with the transition from the monoclinic  $\alpha$  phase below 353 K to the tetragonal  $\beta$  phase above 353 K. For the  $\text{PbSnF}_4$ , this phase transition also marks the temperature at which a change occurs in the slope of the electrical conductivity  $\sigma$  with reciprocal temperature. This is illustrated in Fig. 3 as a plot of  $\log \sigma T$  against  $1/T$ , the data for which have been measured by Chadwick et al. [14]. Above this phase transition in the tetragonal phase, fast ionic transport takes place with activation energies of 0.16–0.17 eV, which is a large reduction from the 0.45–0.52 eV found below the transition in the monoclinic phase [14, 23].

The anomaly in the  $C_{p,m}$  for the  $\text{BaSnF}_4$  occurs in the temperature range where Chadwick et al. [14] found a break in the slope of the electrical conductivity as shown in Fig. 3. Their change in slope occurred around 272 K, yielding very different activation energies above and below the break just as occurred for the  $\text{PbSnF}_4$  salt. Their activation energies for  $\text{BaSnF}_4$  were determined at 0.50 and 0.18 eV for the low- and high-temperature regions, respectively. However, for reasons that are not evident, Denes et al. [15] found the magnitude of the conductivity to be slightly lower than that found by Chadwick et al., but with a nearly linear plot that shows no break around 272 K. Denes et al. detected a tiny change in slope

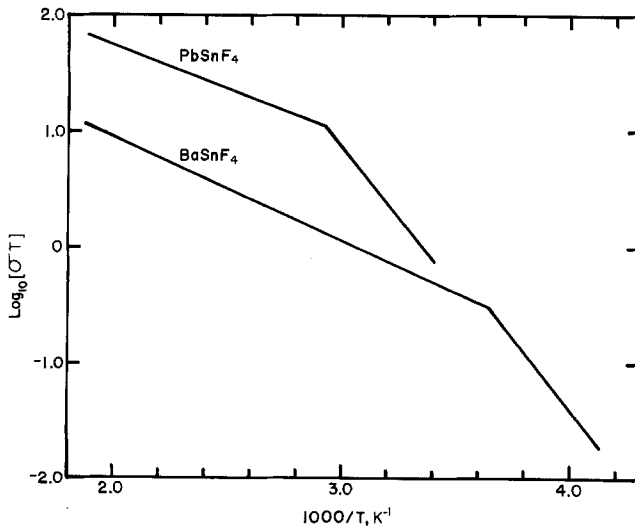


Fig. 3. Logarithm of the quantity  $\sigma T$  for  $\text{PbSnF}_4$  and  $\text{BaSnF}_4$ , where  $\sigma$  is electrical conductivity in  $\text{ohm}^{-1} \cdot \text{cm}^{-1}$  and  $T$  is in K. Data from Ref. 14.



at 400 K, with an activation energy 0.34 eV below 400 K and 0.31 eV above this temperature.

The absence of any phase transition in our heat capacity measurements for  $\text{BaSnF}_4$  is consistent with thermal expansion studies [10, 15]. The lattice constants  $a$  and  $c$  change slowly and linearly without any break or anomalous behavior in the region  $77 < T < 470$  K. However, it is from the nmr experiments by Chadwick et al. [14] that some insight is gained about happenings within the  $\text{BaSnF}_4$  crystal in the region of the  $C_{p,m}$  anomaly  $210 < T < 310$  K.

Their nmr results also confirmed an absence of any phase transition anywhere in the temperature range  $77 < T < 650$  K. They did find that the free induction decay signal consisted of two components which indicate the existence of two nonequivalent sublattices of fluoride ions. One component of their signal was very fast at about  $20 \mu\text{s}$ , which corresponded to a rigid sublattice of  $\text{F}^-$  ions, while the other was a motionally narrowed signal that ranged from  $200 \mu\text{s}$  up to 8 ms depending on the temperature, which corresponded to a mobile sublattice of  $\text{F}^-$  ions. In their model, which provides a qualitative explanation of both the conductivity and the nmr results, the fast-moving  $\text{F}^-$  ions are located on the interstitial sites and moved by direct interstitial jumps. Confirmation of this model requires more detailed structural information than is currently available.

By analogy, structural investigation of the monoclinic  $\alpha$  phase of  $\text{PbSnF}_4$  by Vilminot et al. [23] has shown numerous anionic vacancies which account for the high ionic conductivity in the compound. The modification in the crystal structure to the  $\beta$  tetragonal form results in a decrease in the number of  $\text{F}^-$  ions in the fluorine position which they designated  $\text{F}_1$ . This modification brings about a decrease in the energy barrier without increasing the number of mobile  $\text{F}^-$  ions, leading to the reduction in activation energy from about 0.45 eV in the  $\alpha$  phase to about 0.16 eV in the  $\beta$  phase.

Presumably, a minor shift in the orientation of the  $\text{F}^-$  ions in  $\text{BaSnF}_4$  at about 272 K is similarly responsible for the observed reduction in the activation energy of this compound from 0.50 eV below 272 K to 0.18 eV above this temperature. The  $C_{p,m}/R$  anomaly observed by us from  $210 < T < 310$  K must be associated with a shift in  $\text{F}^-$  ions. Denes et al. [15] carried out  $^{119}\text{Sn}$  Mossbauer spectroscopic experiments to investigate the role in the electrical conductivity of the nonbonded electron pair on Sn(II). They concluded that each nonbonded electron pair is attached strongly to the corresponding tin atom and that there is no possible jump of electron pairs between neighboring tin atoms and thus no electronic conduction due to these electron pairs.

Below 210 K, the  $C_{p,m}/R$  curves for the  $\text{PbSnF}_4$  and  $\text{BaSnF}_4$  in Fig. 1

are similar in shape. The small anomaly found previously in the  $\text{PbSnF}_4$  salt between 130 and 160 K [13] is not present in the  $\text{BaSnF}_4$ . At the lowest temperatures below 20 K, the two curves are compared in Fig. 1 (inset).

## ACKNOWLEDGMENTS

We should like to thank Dr. A. V. Chadwick for preparing the sample and Roey Shaviv for his help in obtaining the heat capacities of the empty calorimeter vessel. One of us (R.D.W.) thanks the Department of National Defence (Canada) for financial support.

## REFERENCES

1. T. H. Etsell and G. S. N. Flengas, *Chem. Rev.* **70**:339 (1970).
2. D. Y. Wang, D. S. Park, J. Griffith, and A. S. Nowick, *Solid State Ionics* **2**:95 (1981).
3. J. M. Reau and J. Portier, in *Solid Electrolytes*, P. Hagenmuller and W. Van Gool, eds. (Academic Press, New York 1978), pp. 313-333.
4. J. M. Reau, C. Lucat, J. Portier, P. Hagenmuller, L. Cot, and S. Vilminot, *Mat. Res. Bull.* **13**:877 (1978).
5. J. Portier, J. M. Reau, S. Matar, J. L. Soubeyroux, and P. Hagenmuller, *Solid State Ionics* **11**:83 (1983).
6. M. S. Frant and J. W. Ross, *Science* **154**:1553 (1966).
7. B. C. Laroy, A. C. Lilly, and C. O. Tiller, *J. Electrochem. Soc.* **120**:12 (1973).
8. J. H. Kennedy and J. C. Hunter, *J. Electrochem. Soc.* **123**:10 (1976).
9. J. D. Donaldson and B. J. Senior, *J. Chem. Soc.* 1821 (1967).
10. J. Pannetier, G. Denes, and J. Lucas, *Mat. Res. Bull.* **14**:627 (1979).
11. G. Perez, S. Vilminot, W. Granier, L. Cot, C. Lucat, J. M. Reau, J. Portier, and P. Hagenmuller, *Mat. Res. Bull.* **15**:587 (1980).
12. P. Claudy, J. M. Letoffe, G. Perez, S. Vilminot, W. Granier, and L. Cot, *J. Fluorine Chem.* **17**:145 (1981).
13. J. E. Callanan, R. D. Weir, and E. F. Westrum, Jr., *Can. J. Chem.* **66**:549 (1988).
14. A. V. Chadwick, E. S. Hamman, D. Van der Putten, and J. H. Strange, *Crystal Latt. Defects Amorph. Mat.* **15**:303 (1987).
15. G. Denes, T. Birchall, M. Sayer, and M. F. Bell, *Solid State Ionics* **13**:213 (1984).
16. G. Denes, J. Pannetier, and J. Lucas, *C.R. Hebd. Seances Acad. Sci.* **C280**(12):831 (1975).
17. E. F. Westrum, Jr., G. T. Furukawa, and J. P. McCullough, *Experimental Thermodynamics, Vol. 1*, J. P. McCullough and D. W. Scott, eds. (Butterworths, London, 1968), p. 133.
18. H. F. Stimson, *J. Res. Natl. Bur. Stand.* **65A**:139 (1961).
19. F. L. McCracken and S. S. Chang, *Rev. Sci. Instrum.* **46**:550 (1975).
20. R. D. Chirico and E. F. Westrum, Jr., *J. Chem. Thermodyn.* **12**:311 (1980).
21. E. F. Westrum, Jr., *Proceedings NATO Advanced Study Institute on Thermochemistry at Viana do Castelo, Portugal*, M. A. V. Ribeiro da Silva, ed. (Reidel, New York, 1984), p. 745.
22. J. T. S. Andrews, P. A. Norton, and E. F. Westrum, Jr., *J. Chem. Thermodyn.* **10**:949 (1978).
23. S. Vilminot, G. Perez, W. Granier, and L. Cot, *Solid State Ionics* **2**:87 (1981).